Assessment of cerebral glucose metabolism in patients with heart failure by ^{18}F-FDG PET/CT imaging

Mingkai Yun, PhD,[a,b] Binbin Nie, PhD,[c] Wanwan Wen,[a,b] Ziwei Zhu,[a,b] Hua Liu, PhD,[c] Shaoping Nie, MD, PhD,[b,d] Rupert Lanzenberger, PhD,[e] Yongxiang Wei, MD, PhD,[a,b] Marcus Hacker, MD,[f] Baoci Shan, PhD,[c] Heinrich R. Schelbert, MD, PhD,[g] Xiang Li, MD, PhD,[a,f] and Xiaoli Zhang, MD, PhD[a,b]

[a] Department of Nuclear Medicine, Laboratory for Molecular Imaging, Beijing Anzhen Hospital, Capital Medical University, Beijing, China
[b] Beijing Key Laboratory of Upper Airway Dysfunction and Related Cardiovascular Diseases, Beijing, China
[c] Division of Nuclear Technology and Applications, Institute of High Energy Physics, Chinese Academy of Sciences, Beijing, China
[d] Division of Emergency & Critical Care Centre, Department of Cardiology, Beijing Anzhen Hospital, Capital Medical University, Beijing, China
[e] Neuroimaging Labs (NIL), Department of Psychiatry and Psychotherapy, Medical University of Vienna, Vienna, Austria
[f] Division of Nuclear Medicine, Department of Biomedical Imaging and Image-guided Therapy, Medical University of Vienna, Vienna, Austria
[g] Department of Molecular and Medical Pharmacology, David Geffen School of Medicine at UCLA, Los Angeles, CA

Received Feb 25, 2020; accepted Jun 10, 2020
doi:10.1007/s12350-020-02258-2

Background. **To evaluate the cerebral metabolism in patients with heart failure (HF).**

Methods. **One hundred and two HF patients were prospectively enrolled, who underwent gated ^{99m}Tc-sestamibi single photon emission computed tomography (SPECT)/CT, cardiac and cerebral ^{18}F-fluorodeoxyglucose (FDG) positron emission tomography (PET)/CT. Fifteen healthy volunteers served as controls. Patients were stratified by extent of hibernating myocardium (HM) and left ventricular ejection fraction (LVEF) into 4 groups where Group1: HM < 10% (n = 33); Group2: HM ≥ 10%, LVEF < 25% (n = 34); Group3: HM ≥ 10%, 25% ≤ LVEF ≤ 40% (n = 16) and Group 4: LVEF > 40% (n = 19). The standardized uptake value (SUV) in the whole brain ($SUV_{whole\text{-}brain}$) and the SUV ratios (SUVR) in 24 cognition-related**

Mingkai Yun and Binbin Nie shared first-authorship

Electronic supplementary material The online version of this article (https://doi.org/10.1007/s12350-020-02258-2) contains supplementary material, which is available to authorized users.

The authors of this article have provided a PowerPoint file, available for download at SpringerLink, which summarises the contents of the paper and is free for re-use at meetings and presentations. Search for the article DOI on SpringerLink.com.

The authors have also provided an audio summary of the article, which is available to download as ESM, or to listen to via the JNC/ASNC Podcast.

All editorial decisions for this article, including selection of reviewers and the final decision, were made by guest editor Nagara Tamaki, MD.

Funding This work was supported by National Natural Science Foundation of China (81871377, 81571717) and Beijing Municipal Science & Technology Comission (Z1 81100001718071).

Reprint requests: Xiaoli Zhang, MD, PhD, Department of Nuclear Medicine, Laboratory for Molecular Imaging, Beijing Anzhen Hospital, Capital Medical University, Beijing, China; *xlzhang68@126.com*

1071-3581/$34.00

brain regions were determined. $SUV_{whole-brain}$ and SUVRs were compared between the 4 patient groups and the healthy controls.

Results. **$SUV_{whole-brain}$ ($r = 0.245$, $P = 0.013$) and SUVRs in frontal areas, hippocampus, and para-hippocampus (r: 0.213 to 0.308, all $P < 0.05$) were correlated with HM. $SUV_{whole-brain}$ differed between four patient groups and the healthy volunteers ($P = 0.016$) and $SUV_{whole-brain}$ in Group 1 was lower than that in healthy volunteers ($P < 0.05$). SUVRs of Group 3 in frontal areas were the highest among four patient subgroups ($P < 0.05$).**

Conclusions. **Cerebral metabolism in the whole brain was reduced but maintained in cognition-related frontal areas in HF patients with HM and moderately impaired global left ventricular function. (J Nucl Cardiol 2022;29:476–88.)**

Key Words: Heart failure • heart–brain axis • ^{18}F-FDG PET • hibernating myocardium

Abbreviations	
HF	Heart failure
PET	Positron emission tomography
CT	Computed tomography
HM	Hibernating myocardium (extent)
SUV	Standardized uptake value
SUVR	SUV normalized for SUV of cerebellum
BMI	Body mass index
MNI	Montreal Neurological Institute
AAL	Automated anatomical labeling

See related editorial, pp. 489–491

INTRODUCTION

Ischemic cardiomyopathy (ICM), as a significant cardiovascular disease (CVD), most frequently originates with obstructive coronary artery disease leading to myocardial injury, which subsequently may lead to an impairment of left ventricular and to heart failure (HF). Remarkably, an interaction between HF and disorders of the brain has been widely recognized in the past decade.[1-4] An increasing number of investigations have proposed that HF might be a pathophysiological factor linked to cognitive impairment.[1,2,5,6] However, the mechanisms underlying functional alterations of the brain after a myocardial infarction are still uncertain and have remained controversial, especially in patients with advanced HF.

Cognition function, structural brain integrity, and heart–brain interactions have been reported as potential players in determining outcomes in patients with CVD and HF.[7-9] The utilization of glucose as the dominant source of brain energy is closely associated with neuronal activity. However, glucose metabolism in the whole brain and cognition-related regions in HF patients remains highly elusive. Although cognitive function-related brain injury including local cerebral blood flow reduction and regional cortical lobe atrophy in HF patients determined by magnetic resonance imaging (MRI) was reported previously.[10,11] A comprehensive functional/physiological analysis of a variety of mediators signal along the heart–brain axis with coordination of physiological processes is still absent. Measurements of the brain glucose metabolism in HF patients might identify an unknown pathophysiologic process and might provide complemental insights into the mechanism of the heart–brain interaction.

Brain [^{18}F] fluorodeoxyglucose (^{18}F-FDG) positron emission tomography (PET) imaging has been extensively used in neurological and psychiatric clinical practice and research to evaluate brain function.[12] Myocardial ^{18}F-FDG PET metabolic imaging, in turn, has become a standard for the assessment of myocardial viability in patients with HF.[13,14] A combination of both cardiac ^{18}F-FDG PET and gated SPECT myocardial perfusion imaging (MPI) can precisely assess the amount of viable ischemic myocardium or hibernating myocardium (HM) and global left ventricular (LV) function. This approach is of essential significant diagnostic and prognostic value in clinical practice.[14-16] Importantly, near-simultaneous evaluation of HM and the brain metabolism by a systematic ^{18}F-FDG PET imaging might help to better understand underlying the heart–brain physiopathology interaction in HF patients.

In this prospective study, we aimed to investigate the metabolic heart–brain interaction in patients with HF, to determine the relationship between cardiac features (HM and global LV function) as well as cerebral metabolic activity in the whole brain, but also in cognition-related regions, as well as additionally to evaluate the global and the regional cerebral metabolic activity in HF patients in comparison with healthy volunteers.

METHODS

Study Population

One hundred and ninety-eight consecutive patients with symptomatic coronary artery disease (CAD) were

prospectively enrolled between June 2016 and September 2017 at Beijing Anzhen hospital for determining myocardial perfusion at rest by ^{99m}Tc-MIBI SPECT/CT MPI and myocardial viability by gated cardiac ^{18}F-FDG PET/CT imaging. Exclusion criteria included an elevated hs-CRP (> 5μmol/L) (n = 33) (in order to exclude presence of a systemic inflammatory process that might influence cerebral FDG uptake), cerebral infarction detectable on PET/CT or history of cerebrovascular disease or mental disease (n = 57), and patients with suboptimal cardiac PET image quality (n = 6) (Figure 1). Fifteen healthy volunteers (age 50(29-58) years, 10 men, BMI 24.5 ± 1.9 kg/m^2) with a low probability (< 5%) of cardiovascular disease (CVD) based on the absence of symptoms and coronary risk factors, a normal physical examination, and a normal resting electrocardiograph (ECG) served as normal controls. This prospective study protocol was approved by the ethics committee of Beijing Anzhen Hospital, Capital Medical University in accordance with the 2013 revision of the Declaration of Helsinki. All participants had given their written informed consent.

Gated ^{99m}Tc-Sestamibi SPECT/CT Myocardial Perfusion Imaging at Rest

Rest gated ^{99m}Tc-MIBI SPECT/CT MPI was performed 90-120 min after injection of ^{99m}Tc-MIBI (740MBq, Chinese Atomic Energy Institute, Beijing, China). Images were acquired for 10 min with a dual-headed Siemens Camera (Siemens Symbia Intevo 16 Systems), equipped with multifocal (SMART ZOOM) collimator. Gated data were acquired with a 20% energy window centered over 140 keV. Gated and non-gated transaxial images were reconstructed with the flash 3D mode and displayed as short axis and horizontal, and vertical long-axis slices.

Cerebral and Gated Cardiac ^{18}F-FDG PET/CT imaging

Within 3 days of the SPECT MPI study, gated ^{18}F-FDG cardiac and cerebral PET/CT metabolic imaging was performed. As previously described,[14,17] patient preparation followed the protocol as outlined in the 2016 ASCN guidelines for PET imaging.[18] After at least 12 h

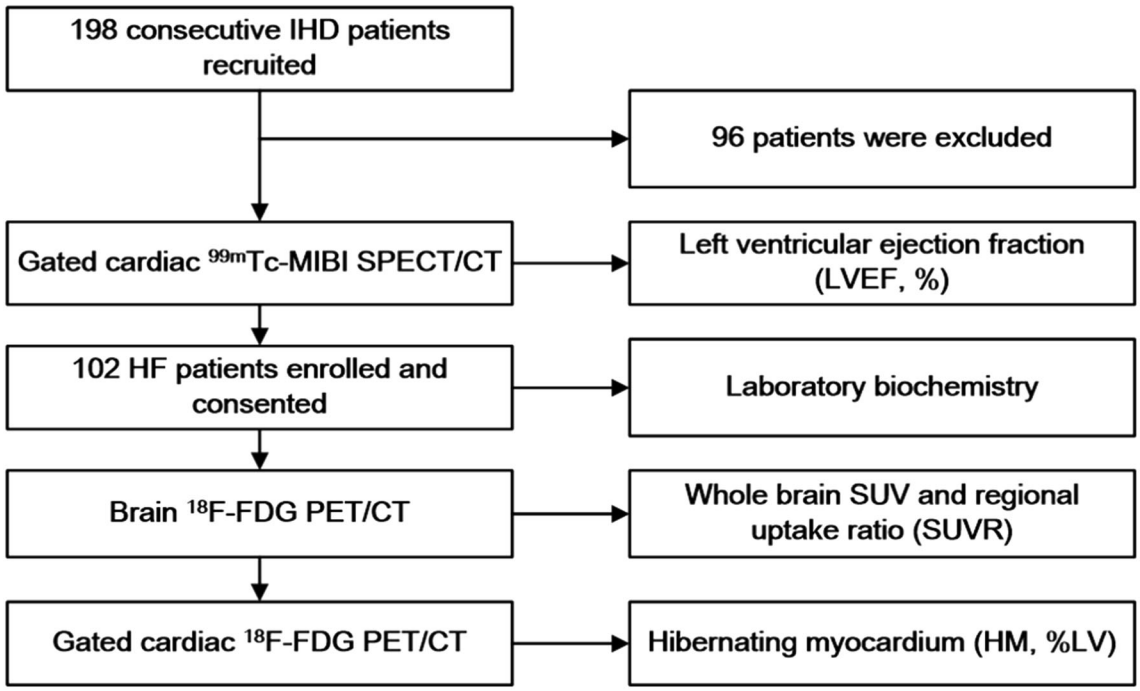

Figure 1. Flow chart of patient disposition. A total of 198 patients with ischemic cardiac disease (IHD); who underwent gated cardiac ^{99m}Tc-sestamibi SPECT/CT MPI at rest, as well as cardiac ^{18}F-FDG PET/CT and brain ^{18}F-FDG PET/CT scans, and 102 eligible heart failure patients were prospectively recruited for this current study. Biochemistry analysis was also performed. LVEF (%) and the extent of hibernating myocardium (HM%), as well as whole brain metabolic activity (SUV) and brain to cerebellum uptake ratio (SUVR) in the specific brain regions were determined by regions of interest (ROI) analysis.

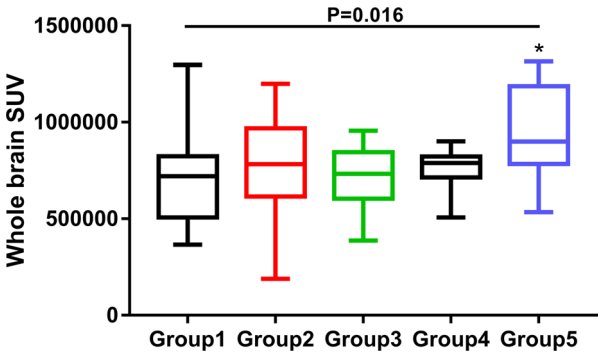

Figure 2. Whole brain metabolic activity (SUV) in the four patient subgroups and in the healthy volunteers (Group 5). A significant difference of $SUV_{whole\text{-}brain}$ brain was observed among four patient subgroups and the healthy volunteers (P = 0.016) *P = 0.007 Group 1 vs. Group 5.

of fasting, the blood glucose level was controlled by oral glucose loading and, if needed, by supplemental iv insulin doses as recommended in the ASNC guidelines. Blood glucose levels averaged 6.57 ± 0.93 mmol/L at the time of the intravenous ^{18}F-FDG (196 ± 28 MBq; Chinese Atomic Energy Institute, Beijing, China) administration.

For cerebral ^{18}F-FDG PET/CT imaging, patients were prepared according to EANM procedure guidelines.[19] Briefly, to allow optimal cerebral imaging, all subjects were positioned comfortably in a quiet and dimly lit room, with sound-proof ear covers to avoid acoustic stimulation. One hour after injection, cerebral ^{18}F-FDG images were acquired for 10 min in 3D mode with a high spatial resolution, whole-body PET scanner (Biograph mCT, Siemens Healthcare), and reconstructed with 5 iterations and 21 subsets to achieve a high spatial resolution. Then, a CT transmission scan (120 kV, 240 mAs) was obtained for attenuation correction. PET images were processed and fused with CT images using the Syngo Applications (Siemens AG, Munich, Germany).

After the brain ^{18}F-FDG PET/CT scan, gated cardiac PET/CT image data were acquired for 10 min. Attenuation correction was performed based on CT data (120 kV, 11 mAs). Image reconstruction employed a point spread function (PSF) + time of flight (TOF) algorithm (TrueX + TOF, UltraHD-PET), with 2 iterations and 21 subsets (Siemens AG, Munich, Germany).

Analysis of Cardiac Gated SPECT/CT and PET/CT Images

Gated SPECT/CT MPI data were transferred to a Siemens e.soft workstation. LV functional parameters, including end-diastolic volume (EDV, mL), end-systolic volume (ESV, mL), and LVEF (%), were calculated by using QGS software (version 3.1, Cedars-Sinai Medical Center, Los Angeles, CA, USA), with manual correction in case of inadequate endocardium and epicardium delineation, especially in patients with severe perfusion defects.

As in our previous investigations,[14,16,17] myocardial perfusion and metabolic activity were assessed by two experienced physicians using the American Heart Association 17-segment and five-point scoring system. Hibernating myocardium (HM) in a perfusion defect was defined as a mismatch score of 1.0 or greater (perfusion score minus FDG score≥1). Scar in a perfusion defect was defined as a mismatch score of less than 1.0 (perfusion score minus FDG score < 1). One segment accounts for 6% of LV; extent of HM (%LV) and the extent of scar (%LV) were calculated from the number of segments with mismatches or matches while the total perfusion defect (TPD, % of left ventricular myocardium) was derived from the number of hypoperfused segments and their defect severity.

Analysis of Cerebral Imaging

The cerebral PET/CT images were pre-processed in SPM12 (Welcome Department of Cognitive Neurology, London, UK). In detail, all cerebral FDG PET images were first standardized into the Montreal Neurological Institute (MNI) space using trilinear interpolation and resampled to 2 × 2 × 2 mm^3 voxels. All the normalized images were then smoothed using an 8 mm^3 full width at half maximum (FWHM) Gaussian kernel. Subsequently, the intracranial tissues of the smoothed images were extracted by the brain mask image in MNI space. The SUV values of all the intracranial voxels were summed up to obtain the whole brain SUV ($SUV_{whole\text{-}brain}$), which was used to reflect the total glucose consumption of brain. Then, 24 cognition-related regions of interest (ROIs) were selected in MNI space using the Automated Anatomical Labeling (AAL) atlas,[20] including all bilateral sub-anatomical regions in frontal area, bilateral hippocampus, bilateral para-hippocampus, and bilateral amygdala (the abbreviation and full name of these 24 brain regions are listed in Suppl. Table 1). These regions were considered to be major cognition-related brain regions, including memory, planning, emotion management, and decision-making executive functions.[21] Finally, the cerebellar region was used as the reference.[22] The SUV_{mean} in the specific cerebral region was divided by the SUV_{mean} of the cerebellum. Thus, the SUVRs of these 24 ROIs were obtained.

Statistical Analysis

The normality of distribution of continuous variables was tested by one-sample Kolmogorov-Smirnov test. Continuous variables with normal distribution were presented as mean ± SD, while non-normally distributed variables as median (interquartile range). The normally distributed data of SUVRs in 24 cognition-related regions in the patients and in healthy volunteers were compared by analysis of variance (ANOVA) followed by post hoc testing (according to the Bonferroni with equal variance assumed or according to the Dunnett's T3 test with equal variance not assumed). The non-normally distributed data of $SUV_{whole\text{-}brain}$ and SUVRs in 24 cognition-related regions in the patients and in healthy volunteers were compared by Kruskal-Wallis test followed by Mann-Whitney U test. Pearson/Spearman correlation coefficients between cerebral metabolism activity ($SUV_{whole\text{-}brain}$ and SUVRs) and cardiac findings (the extent of HM and LVEF) were analyzed for normally/non-normally distributed data. Statistical significance was defined as a $P < 0.05$. Data were analyzed using SPSS software, version 19.0 (SPSS Inc. IBM, Armonk, NY, USA).

RESULTS

Patients

The final study population consisted of 102 patients (95 men, 56.3 ± 9.5 years, BMI 25.8 ± 2.9 kg/m^2) with HF (LVEF: 23.0% (15.0%-37.3%) by gated SPECT. Demographics and clinical findings are summarized in Table 1.

Cerebral Metabolism in Patients Categorized by Viable Ischemic Myocardium and LVEF

Patients were categorized into four subgroups by the extent of HM and LVEF: Group1, patients presenting myocardial scar (HM < 10%/LV, $n = 33$); Group2, patients presenting HM (≥ 10%/LV) with severely impaired LV function (LVEF < 25%, $n = 34$); Group3, patients presenting viability, HM (≥ 10%/LV) and moderately reduced LV function (25% ≤ LVEF ≤ 40%) ($n = 16$); Group 4: patients with relatively preserved ventricular function (LVEF > 40%) ($n = 19$). Fifteen healthy volunteers served as controls (Group 5). As shown in Table 2, LVEF ($P < 0.001$), TPD ($P < 0.001$), extent of HM ($P < 0.001$) and extent of scar ($P < 0.001$) significantly differed between the four patient subgroups. Blood glucose levels at the time of ^{18}F-FDG injection were similar in the patient subgroups (6.54 ± 0.72 mmol/L, 6.67 ± 0.92 mmol/L, 6.52 ± 1. 25 mmol/L, and 6.52 ± 1.05 mmol/L, respectively, $P = 0.910$).

Cerebral Metabolism in Whole Brain and Cognition-Related Regions in Stratified Patients

As shown in Fig. 2 and Table 3, no statistically significant difference of $SUV_{whole\text{-}brain}$ was observed in the four subgroups ($P = 0.424$). However, there was a significant difference in $SUV_{whole\text{-}brain}$ among four subgroups and the healthy volunteers ($P = 0.016$). Specifically, $SUV_{whole\text{-}brain}$ in group 1 patients was significantly lower than in healthy volunteers ($P = 0.007$).

As shown in Fig. 3 and Table 4, SUVRs of the frontal areas, hippocampus, para-hippocampus differed significantly between the four patient groups and healthy volunteers ($P < 0.05$). The regional SUVRs in most of the frontal areas were the highest in Group 3 ($P < 0.05$), while there was no significant difference of SUVRs in amygdala ($P > 0.05$). Furthermore, in comparison with normal volunteers, SUVRs in frontal areas in patients in group 3 were relatively elevated whereas, SUVRs of hippocampus and para-hippocampus in Group 1 were significantly lower ($P < 0.05$). Representative gated ^{99m}Tc-MIBI SPECT/CT myocardial perfusion images at rest, gated cardiac and cerebral ^{18}F-FDG PET/CT images in two patients with HF and different extent of HM and LV dysfunction are shown in Fig. 4.

Correlation between cerebral metabolism with cardiac features

A statistically significant positive relationship between $SUV_{whole\text{-}brain}$ and HM ($r = 0.245$, $P = 0.013$) and a statistically significant negative relationship between $SUV_{whole\text{-}brain}$ and scar ($r = -0.247$, $P = 0.012$) were observed. As shown in Table 5, the SUVRs of bilateral frontal areas, bilateral hippocampus, and bilateral para-hippocampus were significantly associated with the extent of HM (range of r value: 0.213 to 0.308, all $P < 0.05$), but the SUVR of the amygdala was not ($P > 0.05$) (Fig. 5). Furthermore, SUVRs in bilateral frontal regions, bilateral hippocampus, and bilateral para-hippocampus were negatively correlated with the extent of scar (range of r value: − 0.100 to − 0.304, $P < 0.05$). However, there was no significant correlation between SUVRs in these regions and LVEF ($P > 0.05$) and no significant associations were found between cerebral regional SUVRs and high sensitive C-reactive protein (hs-CRP) ($P > 0.05$).

Table 1. Clinical characteristics of the enrolled 102 heart failure patients

Variables	HF patients (*n* = 102)
Age (years)	56.3 ± 9.5
Male (%)	95 (93.1)
New York Heart Association class III - IV (%)	50 (49.0)
Body mass index (kg/m^2)	25.8 ± 2.9
Risk Factors	
Hypertension (%)	37 (36.3)
Diabetes (%)	33 (32.3)
Dyslipidemia (%)	22 (21.6)
Prior and current smokers (%)	78 (76.4)
Coronary artery disease (*n* = 85)	
1-vessel (%)	25 (29.4)
2-veseel (%)	21 (24.7)
3-vessel (%)	39 (45.9)
Laboratory parameters	
BNP > 100 (pg/mL) (%)	73 (71.6)
hs-CRP (μmol/L)	0.78 (0.33 - 2.45)
tHcy (mmol/L)	14.7 (11.1 - 23.0)
Medicine	
Beta-blocker (%)	78 (76.5)
Statin (%)	34 (33.3)
Vasodilators (%)	56 (54.9)
ACEI (%)	25 (24.5)
LV functional parameters by gated SPECT	
LVEF (%)	23.0 (15.0 - 37.3)
EDV (mL)	176.0 (132.0 - 249.0)
ESV (mL)	141.0 (82.0 - 205.5)
^{99m}Tc-MIBI SPECT MPI and ^{18}F-FDG PET/CT	
Total perfusion defect (%, LV)	35.4 ± 15.3
Hibernation Myocardium (%, LV)	12.0 (4.75 - 20.0)
Scar myocardium (%, LV)	19.0 (6.0 - 33.5)

Data are presented as mean ± SD, or *n* (%), or median (interquartile range [IQR])
BNP, brain natriuretic peptide; *hs-CRP,* high-sensitivity C-reactive protein; *tHcy,* total homocysteine; *ACEI,* angiotensin-converting enzyme inhibitor; *LV,* left ventricular; *LVEF,* left ventricular ejection fraction; *EDV,* end-diastolic volume; *ESV,* end-systolic volume

DISCUSSION

The main findings of the current study are as follows: in comparison with the healthy volunteers, the whole-brain metabolic activity ($SUV_{whole\text{-}brain}$) was significantly reduced in HF patients, and relative metabolic activity (SUVR) in specific frontal regions of the brain was elevated in patients with preserved HM and moderately impaired LV function but significantly decreased in patients presenting with myocardial scar.

The Cardiac Function Might Affect the Whole-Brain Metabolism

As the primary source of energy for the brain, glucose metabolism provided by cerebral blood flow could be affected by the cardiac function. Evidence has shown that cerebral blood flow was maintained over a wide range of cardiac output due to a sophisticated autoregulation mechanism of the central nervous system.[23] Thus, to sustain cerebral neuron/neurovascular function, cerebral blood perfusion was relatively constant within a wide range of blood pressure.

Nevertheless, other investigations have demonstrated that impaired cardiac function may directly cause cerebral hypoperfusion, which then could lead to a subsequent loss of cerebral grey matter and to cognitive impairment.[2,10] In the current study, we observed a moderate reduction in whole-brain metabolic activity in patients with both reduced HM and poor LV function in comparison with the healthy volunteers. Previous

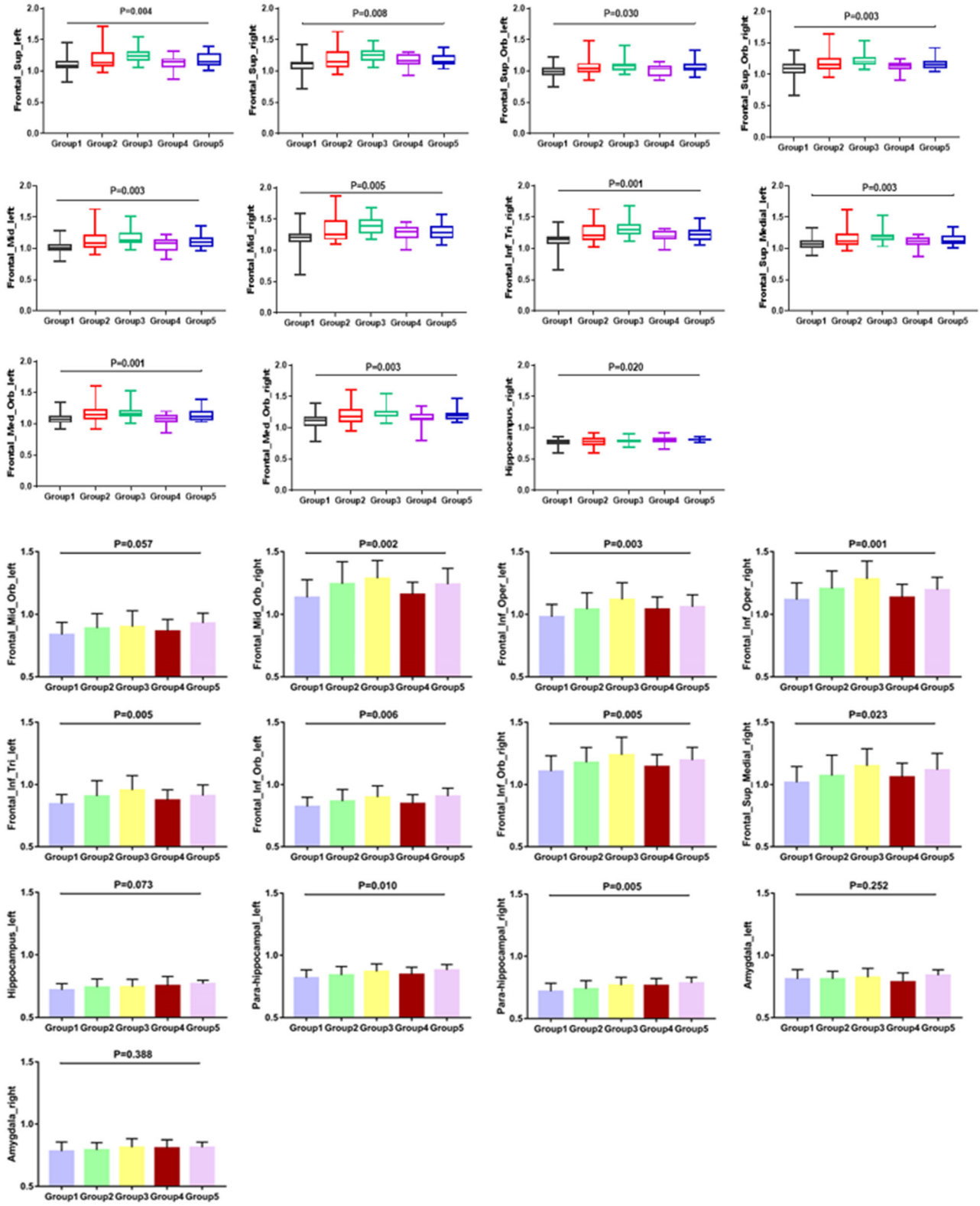

Figure 3. Comparison of the differences of SUVRs of 24 ROIs in four patient subgroups and healthy volunteers.

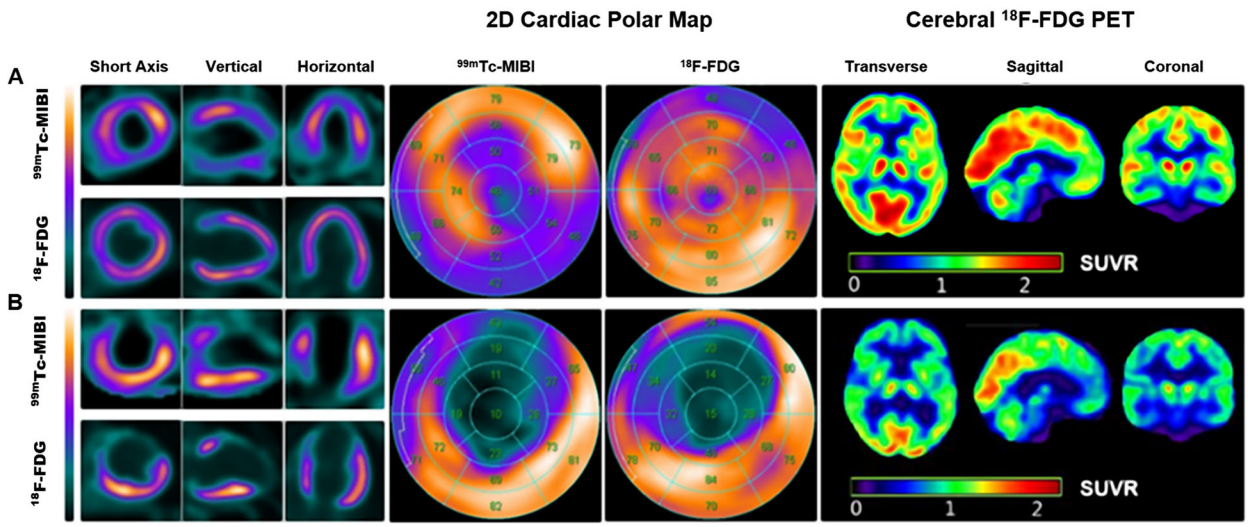

Figure 4. Representative cardiac ^{99m}Tc-MIBI SPECT/CT MPI scan, and cardiac/cerebral ^{18}F-FDG PET/CT scan from two HF patients. (**A**) A 41-year-old man. NYHA: IV. The extent of HM 42%, the extent of the scar was 3%. LVEF was 20%, EDV was 258 mL, and ESV was 207 mL by gated SPECT/CT MPI. ^{18}F-FDG PET/CT scan: $SUV_{whole\text{-}brain}$ 1183475, the cerebral regional SUVR values were 0.89-1.41. (**B**) A 42-year-old man. NYHA: III. The extent of HM 3%, the extent of scar was 57%, LVEF was 15%, EDV was 363 mL and ESV was 307 mL by gated SPECT/CT MPI. ^{18}F-FDG PET/CT scan: $SUV_{whole\text{-}brain}$ was 803869. The cerebral regional SUVR values were 0.84-1.24.

Table 2. Clinical characteristics and imaging parameters in four patient subgroups

Variables	Group1 (n = 33)	Group2 (n = 34)	Group3 (n = 16)	Group4 (n = 19)	P value
Age (years)	56.0(48.5-63.0)	58.0 (51.0-63.3)	59.5 (49.5-62.8)	56.0(48.0-59.0)	0.859
NYHA (III-IV) (%)	25 (75.8)	19 (55.9)	6 (37.5)	0 (0)	0.001
Glucose level at injection (mmol/L)	6.54 ± 0.72	6.67 ± 0.92	6.52 ± 1.25	6.52 ± 1.05	0.910
hs-CRP (μmol/L)	0.46 (0.26-2.50)	0.78 (0.32-2.26)	0.70 (0.36-4.32)	1.01(0.46-3.06)	0.435
BNP (pg/mL)	236.0 (54.00-500.0)	508.5 (238.0-898.8)	151.5 (54.0-283.8)	0.0 (0.0-4.0) ***,†††,‡	<0.001
LVEF by SPECT (%)	19.0 (15.0-28.5)	15.5 (13.8-19.3)	33.0 (28.3-37.8) ***†††	48.0 (43.0-49.0) ***,†††	<0.001
EDV (mL) by SPECT	216.5 (145.8-247.5)	239.5 (187.8-318.3)	143.0 (127.0-210.0) †	110.0 (89.0-125.0)***,†††	<0.001
ESV (mL) by SPECT	166.0 (101.8-206.5)	202.0 (146.0-263.8)	96.0 (83.0-150.0) ††	55.0 (43.0-74.0) ***,†††,‡	<0.001
TPD (%LV)	41.5 ± 15.2	40.5 ± 12.8	33.0 ± 11.3	18.6 ± 10.0***,†††, ‡	<0.001
HM (%LV)	0.0 (0.0-5.5)	20.0 (14.3-25.5) ***	18.0 (12.0-20.0) ***	18.0 (10.0-18.0) ***	<0.001
Scar (%LV)	39.2 ± 15.2	19.1 ± 13. 9***	15.8 ± 11.7***	4.5 ± 7.7***,†‡	<0.001

Data are presented as median (interquartile range [IQR]) or mean ± SD
hs-CRP, high-sensitivity C-reactive protein; *BNP,* brain natriuretic peptide; *LVEF*, left ventricular ejection fraction; *EDV*, end-diastolic volume; *ESV*, end-systolic volume
*** $P < 0.001$, ** $P < 0.01$, * $P < 0.05$ vs. Group 1
††† $P < 0.001$, †† $P < 0.01$, † $P < 0.05$ vs. Group 2
‡‡‡ $P < 0.001$, ‡‡ $P < 0.01$, ‡ $P < 0.05$ vs. Group 3

Table 3. Comparison of the difference of SUVwhole-brain in 4 patients' subgroups and healthy volunteers

	Group 1 (*n* = 33)	Group 2 (*n* = 34)	Group 3 (*n* =16)	Group 4 (*n* = 19)	Group 5 (*n* = 15)	*P* value
$SUV_{whole-brain}$	719652 (507236-823365)	781612 (615619-967713)	783937 (639871-893733)	802558 (748576-872658)	899524 (783282-1186771) *	0.016

Data are presented as median (interquartile range [IQR])
*P = 0.007 vs. Group 1

Table 4. Comparison of the difference of the regional cerebral SUVRs in four patient subgroups and healthy volunteers

Cerebral regions	Group 1 (*n* = 33)	Group 2 (*n* = 34)	Group 3 (*n* = 16)	Group 4 (*n* = 19)	Group 5 (*n* = 15)	*P* value
Frontal_Sup_left	1.08 (1.04-1.16)	1.13 (1.07-1.30)	1.24 (1.16-1.32)**	1.14 (1.05-1.20)	1.15 (1.08-1.28)	0.004
Frontal_Sup_right	1.12 (1.03-1.15)	1.15 (1.06-1.32)	1.24 (1.15-1.32)**	1.16 (1.10-1.26)	1.14 (1.10-1.25)	0.008
Frontal_Sup_Orb_left	0.99 (0.93-1.05)	1.05 (0.97-1.12)	1.08 (1.00-1.11) *	1.03 (0.91-1.09)	1.04 (1.00-1.11)	0.030
Frontal_Sup_Orb_right	1.09 (1.02-1.16)	1.15 (1.07-1.26)	1.20 (1.15-1.27)**	1.14(1.08-1.18)	1.16(1.09-1.21)	0.003
Frontal_Mid_left	1.01 (0.96-1.08)	1.08 (1.00-1.22)	1.13 (1.08-1.25)**	1.08 (0.96-1.14)	1.10 (1.02-1.17)	0.003
Frontal_Mid_right	1.21 (1.13-1.27)	1.25 (1.17-1.49)	1.39 (1.27-1.49)**	1.30 (1.20-1.37)	1.29 (1.20-1.38)	0.005
Frontal_Mid_Orb_left	0.84 ± 0.10	0.89 ± 0.12*	0.90 ± 0.13	0.87 ± 0.10	0.93 ± 0.08**	0.057
Frontal_Mid_Orb_right	1.13 ± 0.14	1.24 ± 0.18**	1.29 ± 0.14**	1.16 ± 0.10†‡	1.24 ± 0.13*	0.002
Frontal_Inf_Oper_left	0.98 ± 0.10	1.04 ± 0.13*	1.12 ± 0.13**†	1.04 ± 0.10	1.06 ± 0.10*	0.003
Frontal_Inf_Oper_right	1.11 ± 0.13	1.20 ± 0.14*	1.28 ± 0.14***	1.13 ± 0.10‡	1.19 ±0.10	<0.001
Frontal_Inf_Tri_left	0.84 ± 0.08	0.91 ± 0.12*	0.96 ± 0.12**	0.87 ± 0.08‡	0.91 ± 0.08*	0.005
Frontal_Inf_Tri_right	1.14 (1.07-1.20)	1.21(1.13-1.38) *	1.30 (1.22-1.39)**	1.20(1.14-1.28)	1.22 (1.13-1.29)	0.001
Frontal_Inf_Orb_left	0.82 ± 0.08	0.87 ± 0.09**	0.90 ± 0.09**	0.85 ± 0.07	0.90 ± 0.06**&	0.006
Frontal_Inf_Orb_right	1.11 ± 0.13	1.18 ± 0.12*	1.24 ± 0.14**	1.14 ± 0.10‡	1.20 ± 0.10*	0.005
Frontal_Sup_Medial_left	1.07 (1.00-1.12)	1.11 (1.04-1.24)	1.19 (1.13-1.23)**	1.12 (1.05-1.18)	1.12 (1.07-1.21)	0.003
Frontal_Sup_Medial_right	1.02 ± 0.13	1.07 ± 0.17	1.15 ± 0.14**	1.06 ± 0.11	1.12 ± 0.13*	0.023
Frontal_Med_Orb_left	1.07 (1.01-1.13)	1.14 (1.07-1.23)*	1.16 (1.12-1.23)**	1.08 (1.02-1.15)†	1.12 (1.06-1.21)	0.001
Frontal_Med_Orb_right	1.11 (1.02-1.17)	1.18 (1.08-1.29)	1.19 (1.17-1.26)**	1.15 (1.11-1.22)	1.19 (1.14-1.24)	0.003
Hippocampus_left	0.72 ± 0.05	0.74 ± 0.07	0.74 ± 0.06	0.75 ± 0.07*	0.77 ± 0.03**	0.073

Table 4 continued

Cerebral regions	Group 1 (n = 33)	Group 2 (n = 34)	Group 3 (n = 16)	Group 4 (n = 19)	Group 5 (n = 15)	P value
Hippocampus_right	0.76 (0.73-0.80)	0.77 (0.72-0.84)	0.78 (0.78-0.81)	0.79(0.77-0.84)	0.81 (0.78-0.83)*	0.020
Para—hippocampus_left	0.82 ± 0.06	0.84 ± 0.07	0.87 ± 0.06**	0.85 ± 0.06	0.88 ± 0.04**†	0.010
Para—hippocampus_right	0.72 ± 0.06	0.74 ± 0.07	0.77 ± 0.06*	0.76 ± 0.06*	0.78 ± 0.05**†	0.005
Amygdala_left	0.81 ± 0.07	0.81 ± 0.06	0.82 ± 0.07	0.79 ± 0.07	0.84 ± 0.05	0.252
Amygdala_right	0.78 ± 0.07	0.79 ± 0.06	0.81 ± 0.07	0.81 ± 0.07	0.81 ± 0.04	0.388

Data are presented as mean ± SD, or n (%), or median (interquartile range [IQR])
Group 1, patients presenting myocardial scar (HM < 10%/LV, n = 33) Group 2, patients presenting HM (≥ 10%/LV) and impaired left ventricular systolic function (LVEF < 25%, n = 34)
Group 3, patients presenting viability, HM (≥ 10%/LV) and moderately preserved left ventricular function (25% ≤ LVEF ≤ 40%) (n = 16)
Group 4: patients with preserved global ventricular function (LVEF > 40%) (n = 19) and Group 5, healthy volunteers serving as controls (n =15)
***P < 0.001, **P < 0.01, *P< 0.05: vs Group1; ††P < 0.01, †P < 0.05: vs Group2
‡P < 0.05: vs Group3; &P < 0.05: vs Group 4

investigations with brain MRI have observed reduced cerebral blood flow and cortical atrophy in HF patients.[10,11] It might thus be possible that cerebrovascular physiological autoregulation mechanisms were no longer fully operational under a sustained severe impairment of cardiac function, resulting in inadequate cerebral blood flow and subsequently metabolic abnormalities.

Effects of cardiac function on the metabolism patterns in the cognition-related cerebral regions

Assessment of the relationship between cardiac metabolism and brain glucose uptake beyond the hemodynamic function was also of great interest. Previous proton magnetic resonance spectroscopy studies in congestive HF patients showed that the metabolite levels in the parietal region were reduced compared with healthy volunteers.[3,8] Recent investigations reported that the enhanced amygdala metabolic activity, which was mainly involved stress, was an independent predictor of major adverse cardiovascular events.[9,24] Reduction of ^{18}F-FDG uptake in cardio-modulatory regions was found in men with impaired LVEF in a recent sex-stratified study, which indicated that a neuroendocrine adaption process occurred as response to myocardial ischemia.[25] By far, there was limited evidence illustrating glucose metabolism in patients with advanced HF.

In clinical practice, a combination of cerebral and cardiac metabolic ^{18}F-FDG PET imaging in patients with HF might provide complementary information on the cerebral physiopathology under conditions of LV dysfunction. Notably, in this study with HF patients in comparison with the healthy volunteers, there was a reduced metabolic activity in the entire brain that was associated with a relatively increased metabolism in frontal brain regions in HF patients with viable HM and moderately impaired global left ventricular function.

In contrast, a trend of reduced glucose metabolism in the entire brain and hippocampus and para-hippocampus was found in patients with reduced HM and LV dysfunction. This heterogeneous metabolic activity in these brain regions is related to a regionally distinct autoregulatory efficiency.[26] The frontal areas as part of neocortex might have a higher autoregulation efficiency and sensitivity than that of archicortex, including the hippocampus and para-hippocampus.[27,28] Hence, there may be a preferential activation of a local compensation process to maintain energy metabolism to a certain extent in frontal areas.

Additionally, no significantly different SUVR in the bilateral amygdala was found between patient subgroups and healthy volunteers. This finding differed from previous studies in patients with suspected or known CAD, that demonstrated a correlation between amygdala metabolic activity and LV dysfunction and perfusion defects in women but not in men.[24] Nevertheless, sex-specific metabolism activity was not assessed in the

Table 5. Spearman correlation coefficients between the SUVRs in 24 ROIs and LVEF, the extent of myocardium scar and the extent of hibernating myocardium (n = 102)

	LVEF (%)		scar (%)		HM (%)	
Cerebral Regions	***r***	***P***	***r***	***P***	***r***	***P***
Frontal_Sup_left	0.065	0.518	-0.153	0.124	0.290*	0.003
Frontal_Sup_right	0.082	0.414	− 0.200*	0.044	0.301*	0.002
Frontal_Sup_Orb_left	0.013	0.900	− 0.110	0.272	0.185	0.062
Frontal_Sup_Orb_right	0.046	0.644	− 0.133	0.183	0.246*	0.013
Frontal_Mid_left	0.044	0.657	− 0.150	0.132	0.271*	0.006
Frontal_Mid_right	0.106	0.291	− 0.182	0.067	0.276*	0.005
Frontal_Mid_Orb_left	0.047	0.640	− 0.100	0.315	0.135	0.178
Frontal_Mid_Orb_right	0.021	0.831	− 0.112	0.263	0.238*	0.016
Frontal_Inf_Oper_left	0.152	0.128	− 0.207*	0.037	0.228*	0.021
Frontal_Inf_Oper_right	0.119	0.848	− 0.177	0.076	0.308*	0.002
Frontal_Inf_Tri_left	0.076	0.448	− 0.187	0.060	0.270*	0.006
Frontal_Inf_Tri_right	0.075	0.453	− 0.201*	0.043	0.306*	0.002
Frontal_Inf_Orb_left	0.085	0.395	− 0.204*	0.040	0.263*	0.008
Frontal_Inf_Orb_right	0.053	0.597	− 0.190	0.055	0.263*	0.008
Frontal_Sup_Medial_left	0.066	0.508	− 0.170	0.088	0.270*	0.006
Frontal_Sup_Medial_right	0.068	0.495	− 0.136	0.172	0.216*	0.030
Frontal_Med_Orb_left	− 0.058	0.559	− 0.111	0.268	0.267*	0.007
Frontal_Med_Orb_right	0.057	0.568	− 0.207*	0.037	0.269*	0.006
Hippocampus_left	0.070	0.485	− 0.221*	0.025	0.213*	0.031
Hippocampus_right	0.082	0.412	− 0.304*	0.002	0.258*	0.009
Para−hippocampus_left	0.063	0.530	− 0.255*	0.010	0.225*	0.023
Para−hippocampus_right	0.126	0.208	− 0.278*	0.005	0.174	0.081
Amygdala_left	- 0.063	0.527	− 0.009	0.927	0.032	0.751
Amygdala_right	0.126	0.206	− 0.214*	0.031	0.136	0.174

SUVR, standardized uptake value ratio; *LVEF*, left ventricular ejection fraction; *HM*, hibernating myocardium
*Significance level of $P < 0.05$

current study because only 7 women (6.9%) were included.

Systematic Inflammation Affecting the Heart–Brain Axis After a Myocardial Ischemia

A recently investigation of Thackeray et al. reported on a possible systemic inflammatory response to an acute myocardial infarction and that involved the heart–brain axis.[29,30] An increased glucose uptake might be related to an activation of microglial cells in the brain triggered by the acute inflammatory response to the myocardial injury. Importantly, hibernating myocardium in humans has been found to actively recruit inflammatory leukocytes leading to further cardiac injury, loss of cardiomyocytes and formation of scar tissue.[31,32]. Thus, a systemic inflammation process associated with the heart–brain axis offers another possible explanation of the relative increase of glucose uptake in cognition-related specific regions of the brain in patients with HM and relatively preserved cardiac function. The presence of HM could be related to the recruitment of inflammatory leukocytes in the infarct territory, and concomitantly elevated cerebral glucose metabolism, while cerebral glucose metabolism declines when HM progressed scar tissue. The underlying implication of regional cerebral immune-metabolic significance needs to be further studied in association with clinical evidence.

NEW KNOWLEDGE GAINED

The cardiac function and metabolism have effects on whole brain glucose uptake and on the metabolism patterns in the cognition-related cerebral regions.

Evaluation of cardiac functional and metabolic features together with brain metabolism by a systematic ^{18}F-FDG PET imaging might contribute to an improved understanding of physiopathological mechanisms underlying the cognitive impairment observed in patients with HF.

Limitations

Firstly, the relatively small sample size in this single-center study might limit the statistical power to draw a meaningful and generalizable conclusion. Secondly, the match between volunteers and patients was only incomplete. There was a significant difference between healthy volunteers and patient groups in age (50(29-58) years vs. 56.0(48.5-63.0) years, 58.0 (51.0-63.3) years, 59.5 (49.5-62.8) years, 56.0(48.0-59.0) years) ($P < 0.05$), while no correlation was found between whole brain metabolism and age in the heart failure cohorts ($r = -0.067$, $P = 0.467$). This age-related change **is very mild** over a 10-year period, though the brain metabolic activity declines with age.[33] Thirdly, the cognitive function of study participants was not evaluated and a connection between chronic cerebral metabolic deficits and the outcome of cognitive impairment was not assessed. Nevertheless, our findings provide metabolic evidence for a heart–brain axis that warrants further long-term follow-up examinations on cerebral structural/metabolic and cognitive function in response to cardiac therapy.

CONCLUSIONS

Cerebral metabolism in the whole brain was reduced but maintained in cognition-related frontal areas in HF patients with HM and moderately impaired global left ventricular function.

Acknowledgement

Michael C. Kreissl, Division of Nuclear Medicine, Department of Radiology and Nuclear Medicine, University Hospital Magdeburg, Magdeburg, Germany for the advice on the manuscript.

Disclosures

The authors declare they have no conflict of interest.

References

1. Cermakova P. Relationship between heart and brain: A new piece of the puzzle. Eur J Heart Fail 2018;20:998-9.
2. Doehner W, Ural D, Haeusler KG, Celutkiene J, Bestetti R, Cavusoglu Y, Pena-Duque MA, Glavas D, Iacoviello M, Laufs U, Alvear RM, Mbakwem A, Piepoli MF, Rosen SD, Tsivgoulis G, Vitale C, Yilmaz MB, Anker SD, Filippatos G, Seferovic P, Coats AJS, Ruschitzka F. Heart and brain interaction in patients with heart failure: Overview and proposal for a taxonomy. A position paper from the study group on heart and brain interaction of the heart failure association. Eur J Heart Fail 2018;20:199-215
3. Kim MS, Kim JJ. Heart and brain interconnection - clinical implications of changes in brain function during heart failure. Circ J 2015;79:942-7.
4. Pressler SJ, Jung M. Chronic heart failure with memory and attention dysfunction: Old problem, thinking anew. JACC Heart Fail 2018;6:593-5.
5. Cardiogenic dementia. Lancet 1977;1:27-28
6. Havakuk O, King KS, Grazette L, Yoon AJ, Fong M, Bregman N, Elkayam U, Kloner RA. Heart failure-induced brain injury. J Am Coll Cardiol 2017;69:1609-16.
7. Zuccala G, Pedone C, Cesari M, Onder G, Pahor M, Marzetti E, Lo Monaco MR, Cocchi A, Carbonin P, Bernabei R. The effects of cognitive impairment on mortality among hospitalized patients with heart failure. Am J Med 2003;115:97-103.
8. Lee CW, Lee JH, Lim TH, Yang HS, Hong MK, Song JK, Park SW, Park SJ, Kim JJ. Prognostic significance of cerebral metabolic abnormalities in patients with congestive heart failure. Circulation 2001;103:2784-7.
9. Tawakol A, Ishai A, Takx RA, Figueroa AL, Ali A, Kaiser Y, Truong QA, Solomon CJ, Calcagno C, Mani V, Tang CY, Mulder WJ, Murrough JW, Hoffmann U, Nahrendorf M, Shin LM, Fayad ZA, Pitman RK. Relation between resting amygdalar activity and cardiovascular events: a longitudinal and cohort study. Lancet 2017;389:834-45.
10. Roy B, Woo MA, Wang DJJ, Fonarow GC, Harper RM, Kumar R. Reduced regional cerebral blood flow in patients with heart failure. Eur J Heart Failure 2017;19:1294-302.
11. Frey A, Sell R, Homola GA, Malsch C, Kraft P, Gunreben I, Morbach C, Alkonyi B, Schmid E, Colonna I, Hofer E, Mullges W, Ertl G, Heuschmann P, Solymosi L, Schmidt R, Stork S, Stoll G. Cognitive deficits and related brain lesions in patients with chronic heart failure. JACC Heart Fail 2018;6:583-92.
12. Varrone A, Asenbaum S, Vander Borght T, Booij J, Nobili F, Nagren K, Darcourt J, Kapucu OL, Tatsch K, Bartenstein P, Van Laere K, European Association of Nuclear Medicine Neuroimaging C. Eanm procedure guidelines for pet brain imaging using [18f]fdg, version 2. Eur J Nucl Med Mol Imaging 2009;36:2103-10
13. Zhang X, Schindler TH, Prior JO, Sayre J, Dahlbom M, Huang SC, Schelbert HR. Blood flow, flow reserve, and glucose utilization in viable and nonviable myocardium in patients with ischemic cardiomyopathy. Eur J Nucl Med Mol Imaging 2013;40:532-41.
14. Zhang X, Liu XJ, Hu S, Schindler TH, Tian Y, He ZX, Gao R, Wu Q, Wei H, Sayre JW, Schelbert HR. Long-term survival of patients with viable and nonviable aneurysms assessed by 99mtc-mibi spect and 18f-fdg pet: A comparative study of medical and surgical treatment. J Nucl Med 2008;49:1288-98.
15. Allman KC, Shaw LJ, Hachamovitch R, Udelson JE. Myocardial viability testing and impact of revascularization on prognosis in patients with coronary artery disease and left ventricular dysfunction: A meta-analysis. J Am Coll Cardiol 2002;39:1151-8.
16. Wang W, Li X, Tian C, Zhao S, Hacker M, Zhang X. Cardiac death in patients with left ventricular aneurysm, remodeling and myocardial viability by gated (99m)tc-mibi spect and gated (18)f-fdg pet. Int J Cardiovasc Imaging 2018;34:485-93.

17. Wei H, Tian C, Schindler TH, Qiu M, Lu M, Shen R, Tian Y, Zhao SH, Zhang X. The impacts of severe perfusion defects, akinetic/dyskinetic segments, and viable myocardium on the accuracy of volumes and lvef measured by gated (9)(9)mtc-mibi spect and gated (1)(8)f-fdg pet in patients with left ventricular aneurysm: Cardiac magnetic resonance imaging as the reference. J Nucl Cardiol 2014;21:1230-44.
18. Dilsizian V, Bacharach SL, Beanlands RS, Bergmann SR, Delbeke D, Dorbala S, Gropler RJ, Knuuti J, Schelbert HR, Travin MI. Asnc imaging guidelines/snmmi procedure standard for positron emission tomography (pet) nuclear cardiology procedures. J Nucl Cardiol 2016;23:1187-226.
19. Varrone A, Asenbaum S, Vander Borght T, Booij J, Nobili F, Nagren K, Darcourt J, Kapucu OL, Tatsch K, Bartenstein P, Van Laere K. Eanm procedure guidelines for pet brain imaging using [f-18]fdg, version 2. Eur J Nucl Med Mol I 2009;36:2103-10.
20. Tzourio-Mazoyer N, Landeau B, Papathanassiou D, Crivello F, Etard O, Delcroix N, Mazoyer B, Joliot M. Automated anatomical labeling of activations in spm using a macroscopic anatomical parcellation of the mni mri single-subject brain. Neuroimage 2002;15:273-89.
21. Leto L, Feola M. Cognitive impairment in heart failure patients. J Geriatr Cardiol 2014;11:316-28.
22. Brown RK, Bohnen NI, Wong KK, Minoshima S, Frey KA. Brain pet in suspected dementia: Patterns of altered fdg metabolism. Radiographics 2014;34:684-701.
23. Paulson OB, Strandgaard S, Edvinsson L. Cerebral autoregulation. Cerebrovasc Brain Metab Rev 1990;2:161-92.
24. Fiechter M, Roggo A, Burger IA, Bengs S, Treyer V, Becker A, Maredziak M, Haider A, Portmann A, Messerli M, Patriki D, Muhlematter UJ, von Felten E, Benz DC, Fuchs TA, Grani C, Pazhenkottil AP, Buechel RR, Kaufmann PA, Gebhard C. Association between resting amygdalar activity and abnormal cardiac function in women and men: A retrospective cohort study. Eur Heart J Cardiovasc Imaging 2019;20:625-32.
25. Fiechter M, Roggo A, Haider A, Bengs S, Burger IA, Maredziak M, Portmann A, Treyer V, Becker AS, Messerli M, Muhlematter UJ, Kudura K, von Felten E, Benz DC, Fuchs TA, Grani C, Pazhenkottil AP, Buechel RR, Kaufmann PA, Gebhard C. Metabolic activity in central neural structures of patients with myocardial injury. J Am Heart Assoc 2019;8:e013070.
26. Horsfield MA, Jara JL, Saeed NP, Panerai RB, Robinson TG. Regional differences in dynamic cerebral autoregulation in the healthy brain assessed by magnetic resonance imaging. PLoS ONE 2013;8:e62588.
27. Henriksen OM, Vestergaard MB, Lindberg U, Aachmann-Andersen NJ, Lisbjerg K, Christensen SJ, Rasmussen P, Olsen NV, Forman JL, Larsson HBW, Law I. Interindividual and regional relationship between cerebral blood flow and glucose metabolism in the resting brain. J Appl Physiol 1985;2018(125):1080-9.
28. Binks AP, Cunningham VJ, Adams L, Banzett RB. Gray matter blood flow change is unevenly distributed during moderate isocapnic hypoxia in humans. J Appl Physiol 1985;2008(104):212-7.
29. Thackeray JT. Imaging the molecular footprints of the heart-brain axis in cardiovascular disease. J Nucl Med 2019;60:728-9.
30. Bascunana P, Hess A, Borchert T, Wang Y, Wollert KC, Bengel FM, Thackeray JT. (11)c-methionine pet identifies astroglia involvement in heart-brain inflammation networking after acute myocardial infarction. J Nucl Med 2020;61(7):977-80.
31. Frangogiannis NG, Shimoni S, Chang SM, Ren G, Shan K, Aggeli C, Reardon MJ, Letsou GV, Espada R, Ramchandani M, Entman ML, Zoghbi WA. Evidence for an active inflammatory process in the hibernating human myocardium. Am J Pathol 2002;160:1425-33.
32. Frangogiannis NG. The pathological basis of myocardial hibernation. Histol Histopathol 2003;18:647-55.
33. Willis MW, Ketter TA, Kimbrell TA, George MS, Herscovitch P, Danielson AL, Benson BE, Post RM. Age, sex and laterality effects on cerebral glucose metabolism in healthy adults. Psychiatry Res 2002;114:23-37.